ACTA IMEKO
ISSN: 2221-870X
June 2025, Volume 14, Number 2, 1 - 9

A GeoAI-based approach for long-term monitoring of urban fabric transformations

Alessandro Vitale[1]

[1] *Department of Civil Engineering, University of Calabria, Via P. Bucci Cubo 45 b, 87036 Rende (CS), Italy*

ABSTRACT
Urban growth has accelerated land use transformations, underscoring the need for accurate and scalable methods to monitor changes over time. This study presents a GeoAI-based methodology to classify and quantify urban fabric transformations over a 24-year period (2000–2024). The methodological framework is applied to the medium-sized municipality of Ravenna, in northern Italy, to evaluate its effectiveness. Landsat 5 and Landsat 9 multispectral images were classified into six Land Use and Land Cover categories using Random Forest (RF) and Support Vector Machine (SVM) algorithms within the Google Earth Engine platform. RF consistently outperformed SVM in both reference years, achieving overall accuracies of 83.8 % (2000) and 86.2 % (2024), with F1-scores exceeding 0.90 for key classes including built-up areas. McNemar's test confirmed the statistical significance of RF's performance advantage. Geospatial analysis revealed a 21.6 % increase in built-up surfaces (+7.8 km²), a 28.6 % increase in grassland/shrubland (+50.4 km²), and a 66.3 % reduction in bareland (−35.0 km²). Urban Density (UD) increased from 4.49 % to 5.73 %, indicating a moderate shift toward more compact urban growth. The results demonstrate the methodology's reliability and transferability, particularly in data-scarce contexts, and provide actionable insights for evidence-based urban planning and sustainable land management.

Section: RESEARCH PAPER

Keywords: GeoAI; remote sensing; land cover mapping; urban fabric transformations monitoring

Citation: A. Vitale, A GeoAI-based approach for long-term monitoring of urban fabric transformations, Acta IMEKO, vol. 14 (2025) no. 2, pp. 1-9. DOI: 10.21014/actaimeko.v14i2.2117

Section Editor: Francesco Lamonaca, University of Calabria, Italy

Received May 12, 2025; **In final form** June 15, 2025; **Published** June 2025

Funding: This research received no external funding.

Corresponding author: Alessandro Vitale, e-mail: alessandro.vitale@unical.it

1. INTRODUCTION

The influence of human activities on environmental dynamics is an important topic in land management research, as it often reflects spatial patterns with both quantitative and qualitative dimensions. Indeed, capturing and analysing how urban and rural landscapes evolve remains complex, primarily due to planners' and decision-makers' spatial and temporal information needs. While practical, traditional approaches such as field surveys and participatory techniques require significant time, financial resources, and human effort.

The emergence of advanced data acquisition technologies and the increasing application of Artificial Intelligence (AI) algorithms have introduced more efficient alternatives for such analysis, enhancing the precision and speed of geospatial evaluations [1], [2]. In particular, progress in geomatics and remotely sensed imagery has transformed the ability to detect and map Land Use and Land Cover (LULC) changes. These technologies offer wide-scale, temporally consistent data that makes them well-suited for analysing natural and built-up environments. The combination of remote sensing and Geographic Information System (GIS) tools has further expanded these capabilities, enabling large-scale studies of LULC transformations [3]-[6].

Nevertheless, processing geospatial data over large areas and long-time spans still present challenges related to computing capacity, data storage, and technical complexity [7]. In response, platforms like Google Earth Engine (GEE) have been developed. GEE provides access to vast satellite archives, such as MODIS, Landsat, and Sentinel, and enables fast cloud-based processing for tasks like image classification. It also allows integration of machine learning algorithms and includes built-in storage, making it a robust solution for managing and analysing geospatial data [8]-[10].

Among the machine learning techniques applied in LULC classification, Random Forest (RF) and Support Vector

Machine (SVM) have shown robust performance. SVM, for instance, has reached 90.8 % accuracy for paddy rice classification in China [11] and 93.8 % accuracy when applied to Sentinel-2 data in India's Munneru River Basin [12]. RF has often outperformed SVM, with studies reporting classification accuracies of 95.2 % using Landsat 9 imagery [13].

While GeoAI methodologies are widely acknowledged for their effectiveness, their real value is particularly evident in areas where comprehensive, high-resolution cartographic data are scarce or unavailable. Traditional land cover maps, such as those produced by authoritative sources like CORINE, frequently suffer from coarse resolutions and infrequent updating cycles, rendering them insufficient for detailed urban fabric transformation monitoring. In such contexts, GeoAI-based workflows become indispensable, allowing for consistent and high-resolution land monitoring and management even in the absence of robust ancillary data [14].

This study presents a GeoAI-driven methodology that employs these innovative approaches to measure and monitor urban fabric transformations in Ravenna, Italy, over a 24-year period (2000–2024). The workflow integrates Landsat multispectral satellite imagery processed within the GEE environment, employing RF and SVM algorithms to classify land use and land cover into six distinct classes. A comparative analysis between RF and SVM is conducted to determine the most accurate classifier for reliably capturing urban transformations.

The primary objective of this research is to validate the efficacy, scalability, and transferability of integrating GeoAI and open-source cloud platforms for systematic monitoring of long-term urban fabric changes. This research contributes to the evolving field of geomatics, where the integration of Earth Observation (EO) data and AI-driven methods enables advanced analysis of urban transformation patterns. Specifically, the study addresses the following questions:

1. Can the integration of GeoAI methodologies enhance the precision and scalability of urban transformation monitoring, especially in the absence of detailed reference cartography?
2. How does the performance of RF compare to SVM in accurately classifying complex urban landscapes over extended temporal scales?

The remainder of the paper is structured as follows: Section 2 presents the study area and detailed methodology, including theoretical considerations and validation procedures. Section 3 reports classification results and the analysis of urban transformations using the Urban Density indicator and Urban Morphological Zones. Section 4 discusses implications, comparative analyses with regional urbanisation trends, methodological strengths, and limitations. Section 5 concludes by summarizing key findings, contributions to GeoAI methodologies, and future research directions.

2. MATERIALS AND METHODS

2.1. Study Area

To test the effectiveness of the proposed methodology, the city of Ravenna was selected as a case study. Located in the Emilia-Romagna region, in Northern Italy, Ravenna is a small to medium-sized municipality with a population of approximately 157,277 inhabitants and a total area of around 629 km² (Figure 1).

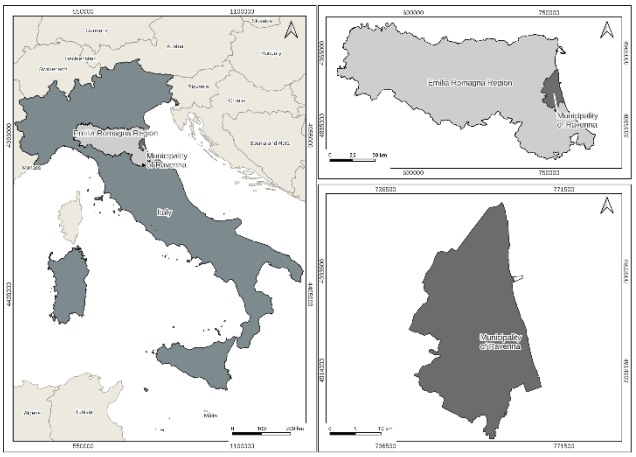

Figure 1. Geographic location of the study area.

The well-preserved historical core, among UNESCO World Heritage Sites, is a dense, compact urban nucleus that contrasts sharply with the peripheral areas, which have undergone substantial expansion and transformation over the past two decades. Notably, growth has occurred in the industrial zones near the Adriatic coast and port infrastructure, as well as in the surrounding residential areas. These spatial dynamics have led to a complex urban morphology, where consolidated historical areas coexist with newer, more fragmented urban developments.

Such contrasts make Ravenna an ideal setting for testing the proposed GeoAI-based methodology.

To support the classification and analysis of urban transformations, the study area was subdivided into several morphological zones based on the definitions provided by the Municipal Structural Plan (PSM). These include the historical urban core, suburban residential expansions, peripheral industrial areas, and dispersed residential settlements.

2.2. Dataset Description

The spatial framework for this study was derived from the PSM, which provided a reference for analysing the distribution and transformation of built-up areas in Ravenna over 24 years. Based on this reference, as introduced in the section 2.1, several urban morphological zones were delineated and monitored by classifying multi-temporal multispectral satellite imagery using two supervised machine learning algorithms: RF and SVM.

The study used remotely sensed data from Landsat 5 and Landsat 9 missions to investigate urban fabric changes between 2000 and 2024.

All satellite imagery was processed and analysed within the GEE cloud-based environment. For 2000, Level 2, Collection 2, Tier 1 data from Landsat 5 (Thematic Mapper) were used. These images offer atmospherically corrected surface reflectance and land surface temperature products. With a 30-meter spatial resolution, the dataset includes four visible and near-infrared (VNIR) spectrum bands and two short-wave infrared (SWIR) bands. The images were orthorectified to ensure spatial accuracy in detecting built-up areas and mapping land cover patterns at the beginning of the study period.

For 2024, Landsat 9 imagery was employed. This dataset includes 11 spectral bands spanning the visible, NIR, and SWIR regions, with improved spectral sensitivity and radiometric resolution.

2.3. Data Preprocessing

All satellite datasets underwent a rigorous preprocessing and standardisation workflow to enable consistent and temporally accurate LULC changes in Ravenna between 2000 and 2024, reflecting standard practices in geomatics for the spatial harmonization of multi-temporal EO datasets. This phase was critical to address the variability between Landsat missions, such as differences in sensor characteristics, atmospheric conditions, and acquisition geometry, which can otherwise introduce inconsistencies in multi-temporal classifications.

Preprocessing was conducted using the GEE cloud platform. As an open-access, cloud-based environment, GEE supports a fully integrated and reproducible remote sensing workflow, from image selection to classification. Furthermore, it ensures compatibility with GIS platforms, allowing classified outputs to be exported and analysed in a spatial decision-making context.

For this study, Level-2, Collection 2 surface reflectance products were selected for both Landsat 5 (year 2000) and Landsat 9 (year 2024). These datasets include atmospheric corrections and standardised surface reflectance values, minimising spectral discrepancies caused by sun angle and atmospheric variation. Only satellite images with less than 10 % cloud cover were considered, and cloud masking was applied using the Quality Assurance (QA) bands. For each year, a median composite was generated from the filtered images, spanning 1 January to 31 December for 2000, and 1 January to 30 September for 2024, thereby reducing residual noise and seasonal anomalies.

All images were geometrically corrected and reprojected into the WGS 84/UTM Zone 32N coordinate reference system to ensure spatial consistency across both datasets. This reprojection was essential for aligning pixel locations and ensuring that classification outputs from both years were spatially comparable. As all Landsat datasets used in this study share a native resolution of 30 metres, no further resampling was required.

The presented preprocessing strategy, encompassing atmospheric correction, geometric standardisation, temporal filtering, and radiometric harmonisation, prepares the satellite data for accurate, uniform classification across time, guarantees spatial and spectral consistency, and supports the reliable detection of long-term urban fabric transformations.

2.4. Classification of Multispectral Satellite Imagery

This study adopts a methodological framework for the automatic classification of multispectral satellite imagery to evaluate and compare the performance of two supervised machine learning algorithms: RF and SVM. Both classifiers were implemented within the GEE platform. The classification was conducted to map six LULC classes across the years 2000 and 2024.

The six defined LULC categories are listed and described in Table 1 and include: tree cover, grassland and shrubland, agricultural areas, water bodies, built-up surfaces, and bareland.

A total of 1,498 labelled samples were manually digitised directly on the satellite imagery to support supervised classification. These samples were selected by expert photointerpretation using false-colour and natural-colour composites to ensure spectral representativeness and thematic consistency. The sample distribution was stratified across all six classes to ensure balanced coverage. Each point was positioned using WGS 84 / UTM Zone 32N, ensuring accurate geolocation and spatial consistency between training data, classification outputs, and GIS-based urban analysis layers.

Table 1. Description of LULC classes.

LULC Class	Description
Water (W)	Natural or artificial water bodies, including rivers, lakes, ponds, and reservoirs.
Tree Cover (TC)	Areas with dense tree canopy, such as forests and managed plantations.
Grassland and Shrubland (G/S)	Open landscapes with grasses, shrubs, or sparse vegetation, often transitional zones.
Agricultural (A)	Cultivated land used for crops, orchards, and other agricultural purposes.
Built-up (B)	Urban areas with man-made structures, including residential, industrial, and infrastructure zones.
Bareland (Bar)	Exposed soils, rocky terrain, or degraded land with minimal vegetation cover.

Of the full dataset, 70 % (1,032 samples) were randomly allocated to train the classifiers, while 30 % (466 samples) were reserved for independent validation. Each ground truth point was assigned a numeric class label and stored in a single feature collection within the GEE environment.

The classification process involved sampling the spectral band values at each training point to generate feature vectors, which were then used by RF and SVM to learn class-specific decision rules. These trained classifiers were subsequently applied to the entire multispectral image mosaic, generating pixel-based classification maps for both reference years.

2.5. Random Forest (RF) Classifier

RF is a widely used ensemble-based supervised learning algorithm, particularly suitable for remote sensing applications such as LULC classification and the spatial analysis and monitoring of urban fabric transformations.

The algorithm operates by constructing multiple independent decision trees during the training phase. Each tree is built using a random subset of the training data and a random selection of input features (e.g., spectral bands), contributing to model robustness and reducing overfitting.

Among the key parameters that influence RF performance, the number of decision trees (also referred to as estimators) plays a central role. Increasing the number of trees typically enhances classification accuracy by reducing model variance and stabilising predictions [15]-[17]. In this study, the RF model was configured with 100 trees, a value chosen to optimise predictive performance while maintaining computational efficiency within the GEE environment.

2.6. Support Vector Machine (SVM) Classifier

SVM is a supervised learning algorithm widely adopted in remote sensing for classifying multispectral satellite imagery. Its use in LULC classification applications has proven effective, particularly in cases where accurate measurement and monitoring of class boundaries in complex spatial datasets are required.

SVM functions by identifying an optimal separating hyperplane that maximises the margin between two distinct classes. This margin is defined as the distance between the hyperplane and the closest data points from each class, known as support vectors. Through this mechanism, SVM provides a precise and mathematically grounded method for discriminating between land cover types, contributing to the accurate quantification of spatial transformations.

Several core parameters influence SVM's classification performance. The kernel function determines how the algorithm handles data not linearly separable in the input feature space, enabling flexible modelling of complex relationships. The C parameter is a regularisation factor, balancing the trade-off between achieving a low classification error on the training set and maintaining a wide margin between classes. The gamma parameter controls the influence of individual training samples, shaping how far each data point can affect the decision boundary.

In this study, the SVM classifier was implemented using the default parameters in GEE: a radial basis function (RBF) kernel, a regularization parameter value of 1, and a gamma value automatically set to the inverse of the number of input features. These settings ensure generalizability while minimizing the need for manual tuning in the absence of prior class-specific parameter optimization.

2.7. Classification Performance Measurement

The performance of LULC classification models is influenced by multiple factors, including the volume and distribution of training data, the characteristics of the study area, and the spectral and radiometric properties of the satellite imagery employed. Prior research has demonstrated varying levels of classification accuracy when applying different machine learning techniques to Landsat 5 and Landsat 9 datasets [18]-[20]. These studies reinforce the importance of rigorous validation procedures to ensure the reliability of classification outcomes.

In this study, classifier performance was assessed using two key statistical indicators derived from the confusion matrix: Overall Accuracy (OA) and F1-score (F1). OA quantifies the proportion of correctly classified pixels across the entire dataset and is expressed as:

$$OA = \frac{Correctly\ Classified\ Pixels}{Total\ Pixels} \times 100\,, \tag{1}$$

F1-score represents the harmonic mean of precision and recall (producer accuracy), providing a balanced evaluation of classification quality per class. It is calculated as:

$$Precision = \frac{TP}{TP + FP} \times 100\,, \tag{2}$$

$$Recall = \frac{TP}{TP + FN} \times 100\,, \tag{3}$$

$$F1 - score = \left(\frac{2 \cdot PrecisionRecall}{Precision + Recall}\right), \tag{4}$$

where:

- TP (True Positives) are instances correctly predicted as belonging to a class;
- FN (False Negatives) are instances belonging to a class but misclassified as another;
- FP (False Positives) are instances incorrectly predicted as belonging to a class when they do not.

F1-score was adopted in this study as the primary metric for per-class performance evaluation, as it balances both omission and commission errors and is better suited for assessing classifier performance in classes with potentially imbalanced distributions.

Table 2. Structure of the 2 × 2 contingency table for McNemar's test.

	SVM Correct	SVM Incorrect
RF Correct	a	b
RF Incorrect	c	d

To complement these conventional metrics, McNemar's test was introduced to statistically assess the significance of differences between classifier performances.

This non-parametric statistical test compares two paired classification outputs and evaluates whether their discrepancies are statistically significative.

The test is based on a 2 × 2 contingency table structured as in Table 2.

It focuses on the discordant predictions (b and c) and uses the following chi-squared statistic:

$$\chi^2 = \frac{(b - c)^2}{b + c}, \tag{5}$$

If $b + c < 25$, an exact binomial test is preferred.

A $p < 0.05$ indicates a statistically significant difference between classifiers.

In this study, McNemar's test was applied to the complete validation datasets for 2000 and 2024, and per LULC class. This allowed a more detailed assessment of each classifier's strengths and weaknesses, particularly in challenging or spectrally ambiguous categories such as bareland and grassland/shrubland.

2.8. GIS-Based Measurement of Urban Fabric Transformations

Following the LULC classification for the years 2000 and 2024, the resulting built-up maps were imported into a GIS environment for post-processing and spatial analysis. The primary goal of this stage was to quantify the evolution of built-up areas over the 24-year period and to assess the spatial dynamics of urban expansion across the municipality of Ravenna.

As a first step, the Urban Density (UD) indicator was computed to measure the overall intensity of urbanisation at the municipal scale. This metric quantifies the share of the municipality's total area that is classified as built-up in each reference year, providing a synthetic yet robust measure of urban compactness.

The urban density was calculated using the following functional form:

$$Urban\ Density\ (UD) = \frac{A_{\mathrm{BU}}}{A_{\mathrm{TOT}}}, \tag{6}$$

where:

- A_{BU} is the total surface area classified as built-up in the year considered (2000 or 2024);
- A_{TOT} is the total administrative area of the municipality of Ravenna.

The UD indicator captures the global urbanisation trend, highlighting whether built-up surfaces have become more compact or dispersed over time at the citywide scale. However, to investigate the spatial variability of urban growth, a more detailed morphological classification was required.

The analysis was further refined by delineating specific Urban Morphological Zones (UMZs) to evaluate the transformation of the urban fabric. These zones were defined using reference cartographic data provided by the geoportal of

the Emilia-Romagna Region and aligned with the city's PSM. The reference year 2000 served as the baseline for measuring spatial growth and transformation dynamics.

The city of Ravenna was subdivided into four UMZs based on its structural and functional characteristics:

- Core Urban Zone: The historic centre and high-density residential and service areas.
- Suburban Zones: Residential expansions developed outward from the urban core.
- Peripheral Areas: Low-density, recent developments including industrial sectors, port-related infrastructure, and coastal residential settlements.
- Residential Isolated Structures: Dispersed built-up forms in rural or semi-rural contexts, characterised by fragmentation and spatial discontinuity.

Built-up surfaces were extracted from the classification outputs for each reference year and overlaid on the UMZ boundaries. This allowed for a spatially disaggregated assessment of urban expansion, capturing both absolute changes in built-up area and the directionality of growth.

This dual-scale analytical framework, integrating global urban density and local morphological classification, enabled the study to distinguish between different development patterns, including urban consolidation, edge expansion, and fragmented sprawl. It provides a robust basis for understanding how Ravenna's urban structure has evolved over the past two decades and for supporting future land management strategies.

3. RESULTS

3.1. Performance Comparison of RF and SVM Classifiers

The classification results for the RF and SVM models were evaluated for the years 2000 and 2024 using OA and class-specific F1-scores. These metrics provide a robust basis for assessing each classifier's ability to reliably measure LULC types in a complex urban landscape.

As shown in Table 3, the RF model outperformed SVM in both years and across all LULC classes. In 2000, RF achieved an OA of 0.83, compared to 0.64 for SVM. In 2024, RF's OA improved further to 0.86, while SVM reached 0.70.

The RF model consistently delivered high F1-scores for the Water, Tree Cover, and Built-up classes in both years, with values above 0.88. Notably, the Built-up class was classified with high reliability by both RF and SVM, with F1-scores of 0.92 (2000) and 0.90 (2024) for RF, and 0.85 (2000) and 0.83 (2024) for SVM. This consistent performance across models and years justifies the use of the built-up class for detailed spatial analysis of urban fabric transformations.

Other land cover classes, such as agricultural and grassland/shrubland, showed moderate F1-scores for both classifiers, with RF achieving notably better results. For example, RF recorded 0.87 for grassland/shrubland in 2024, while SVM achieved 0.78. The most challenging class for both models remained bareland, though RF improved its F1-score from 0.68 (2000) to 0.78 (2024), whereas SVM struggled to exceed 0.50 in either year (Figure 2).

These results confirm RF's superior performance in detecting diverse land cover types, especially those with complex spectral characteristics. The built-up class, central to this study's spatial and morphological analysis, was accurately and consistently detected across classifiers and years, ensuring the reliability of the transformation assessment in the subsequent sections.

Table 3. Per-class F1-scores and Overall Accuracy (OA) for RF and SVM classifiers in 2000 and 2024.

Class	RF 2000	SVM 2000	RF 2024	SVM 2024
W	0.97	0.87	0.97	0.96
TC	0.95	0.65	0.88	0.60
GS	0.75	0.20	0.87	0.78
A	0.79	0.70	0.80	0.75
B	0.92	0.85	0.90	0.83
Bar	0.68	0.30	0.78	0.50
Overall Accuracy (OA)	**0.83**	**0.64**	**0.86**	**0.70**

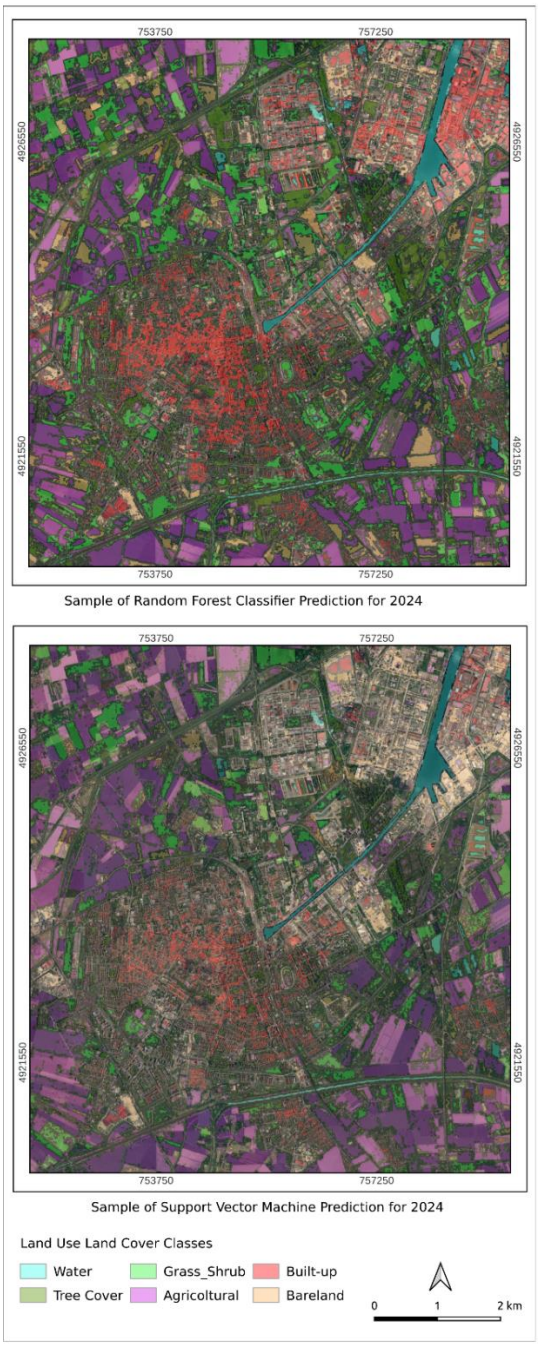

Figure 2. Visual comparison of land use and land cover classifications for 2024 using RF and SVM algorithms.

Table 4. McNemar's 2 × 2 contingency table comparing RF and SVM classification results for 2000.

	SVM Correct	SVM Incorrect
RF Correct	280	108
RF Incorrect	15	60

Table 5. McNemar's 2 × 2 contingency table comparing RF and SVM classification results for 2024.

	SVM Correct	SVM Incorrect
RF Correct	323	76
RF Incorrect	28	36

To further validate these performance differences, McNemar's test was applied to the classification outputs for 2000 and 2024. This test evaluates whether the disagreement between RF and SVM predictions is statistically significant. The results confirmed that RF's improvements over SVM are not due to chance.

Table 4 represents the contingency table for 2000, in which $b + c = 123$. For this reason, the chi-squared approximation was used, resulting in $\chi^2 = 67.40$, $p < 2.7 \cdot 10^{-18}$.

Table 5 represents the contingency table for 2024, in which $b + c = 104$. The chi-squared approximation was used, resulting in $\chi^2 = 18.10$, $p < 2.7 \cdot 10^{-6}$.

These results statistically prove the F1-score findings and justify the use of RF classification outputs, particularly for the built-up class, in long-term monitoring and urban analysis applications in Ravenna. Notably, the built-up class was consistently well-classified by both models, but the difference in performance between RF and SVM remains statistically significant according to McNemar's test. Therefore, to ensure the highest reliability in evaluating built-up area dynamics, only the RF-derived classifications were used in the spatial and temporal analysis of urban fabric transformations presented in the following sections.

3.2. Quantitative Analysis of Urban Fabric Transformations

The measurement of LULC changes in Ravenna between 2000 and 2024 reveals significant transformations in the spatial configuration of the urban fabric. Classification outputs generated through the RF model and processed within a GIS environment provided the basis for a comparative evaluation of surface coverage changes across six defined LULC categories. These results offer detailed insights into the direction and intensity of urban expansion and environmental transitions over the 24-year period.

As shown in Table 6, the built-up class increased by 7.8 km² (+21.6 %), confirming a steady trend of urbanisation in the municipality. To characterise this trend more broadly, the UD indicator was calculated as the ratio between the total built-up area and the municipal territory. In Ravenna, increased from 4.49 % in 2000 to 5.73 % in 2024, indicating a moderate but measurable intensification of urban land consumption.

This represents a shift toward a more compact urban form at the municipal scale. While these values remain below national averages for Northern Italy in the same period (e.g., ~7 % in 2000), they suggest a relatively contained and structured pattern of urban growth in Ravenna compared to the more dispersed development observed in surrounding regions.

Table 6 presents the computed surface areas and percentage distributions of each LULC class for both reference years.

Table 6. Measured surface area and percentage changes in LULC classes for 2000 and 2024.

LULC Class	2000 (km²)	2024 (km²)	2000 (%)	2024 (%)	Δ Area (km²)	Δ (%)
W	32.0	34.2	5.1	5.4	+2.2	+6.4
TC	96.1	82.8	15.2	13.1	-13.3	-16.1
GS	126.0	176.4	20.0	28.0	+50.4	+28.6
A	259.6	247.5	41.2	39.4	-12.1	-4.9
B	28.3	36.1	4.5	5.8	+7.8	+21.6
Bar	87.8	52.8	14.0	8.4	-35.0	-66.3
Total	**629.8**	**629.8**	**100**	**100**	**0**	-

Water bodies increased by 2.2 km² (+6.4 %), likely due to better detection or physical expansion. Tree cover declined by 13.3 km² (−16.1 %), mostly in peripheral areas, reflecting deforestation or land conversion. Conversely, grassland and shrubland expanded by 50.4 km² (+28.6 %), potentially from land abandonment or ecological succession. Agricultural land decreased by 12.1 km² (−4.9 %), largely replaced by built-up surfaces or natural vegetation. The most notable decline was in bareland, which shrank by 35.0 km² (−66.3 %), suggesting increased land reuse or vegetation recovery.

To interpret the spatial structure of these transformations, the built-up class was further analysed across the four Urban Morphological Zones (UMZs) defined in the methodological framework: Core Urban Zone, Suburban Zones, Peripheral Areas, and Residential Isolated Structures.

In the Core Urban Zone, encompassing Ravenna's historic centre, urban densification was evident. Underutilised plots were infilled with medium-density housing and services, aligning with policy goals of urban consolidation and heritage preservation.

Suburban and peripheral zones experienced significant growth in built-up area (Figure 3). These zones absorbed much of the residential and port-related expansion, especially along the Adriatic corridor, with low-to-medium-density housing and logistical infrastructure. This growth reflects Ravenna's planned extension of productive and residential functions in its urban edge.

In contrast, isolated residential structures in rural surroundings expanded more diffusely, contributing to a fragmented urban pattern. Although partly driven by lifestyle and housing demand, this form of development raises challenges in terms of service provision, land efficiency, and environmental sustainability.

Taken together, these observations confirm that Ravenna's urban evolution between 2000 and 2024 was marked by both quantitative expansion and internal reorganisation. The integration of the Urban Density indicator with UMZ-based spatial analysis allowed for a dual-scale interpretation: one that highlights a moderately intensifying urban core and planned edge growth, while still acknowledging signs of spatial fragmentation in outlying areas. The applied methodology, combining remote sensing, machine learning, and spatial zoning, proves effective in quantifying urban dynamics and supporting long-term monitoring strategies.

4. DISCUSSION

The comparative analysis of classification performance confirmed that RF algorithm delivers more accurate and reliable measurements of LULC changes in Ravenna than the SVM

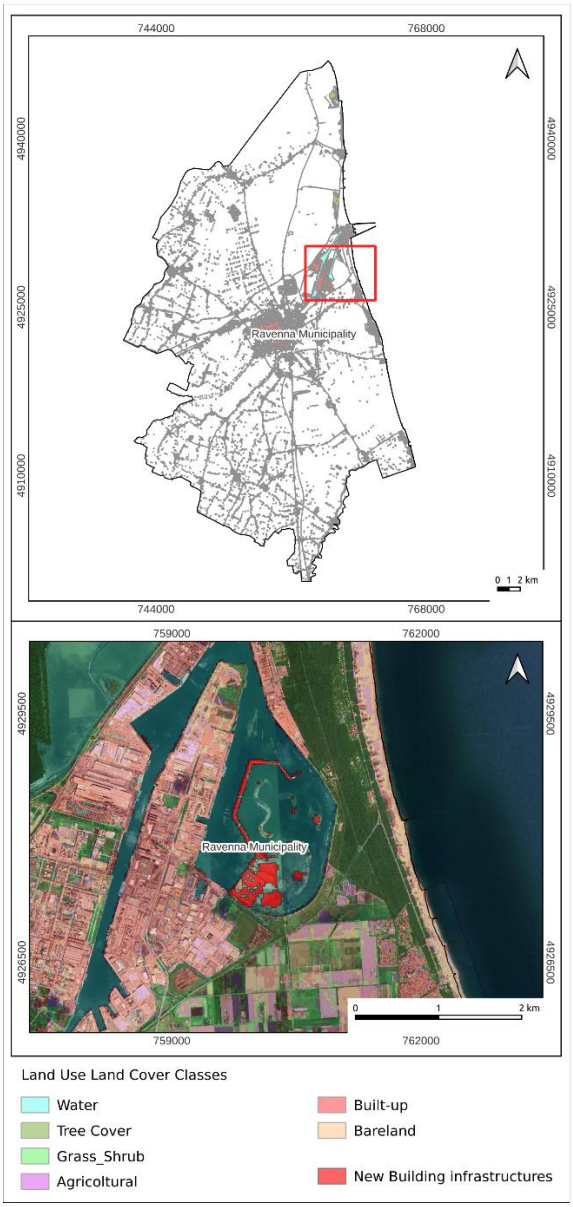

Figure 3. Example output of the classification-based methodology: measured increase in built-up areas within suburban and peripheral zones between 2000 and 2024.

model. RF achieved an OA of 83 % in 2000 and 86 % in 2024, reflecting consistent and high-fidelity measurement of spatial patterns over time. Furthermore, RF recorded F1-scores exceeding 0.90 for key urban and natural classes such as water, built-up areas, and tree cover, underscoring its robustness in classifying distinct features in rapidly evolving urban environments.

In contrast, the SVM classifier yielded an OA of 64 % in 2000 and 70 % in 2024, indicating a more limited capacity to capture the spectral variability of complex landscapes. Particularly in spectrally ambiguous classes such as bareland and grassland/shrubland, SVM's performance was significantly lower, with F1-scores falling below 0.50 in 2000. These results are consistent with prior studies [21], which highlight RF's advantage in modelling non-linear relationships and handling mixed land cover classes more effectively.

Beyond numerical differences, these findings were formally validated through McNemar's test, which demonstrated that the performance advantage of RF over SVM is statistically significant in both years. For 2000 and 2024, the test yielded p-values far below the 0.05 threshold, confirming that RF's higher classification accuracy is not due to chance. This statistical evidence applies across all classes, including built-up, which is central to the urban fabric transformation analysis.

The study shows how GeoAI methods, when integrated into an open-source cloud platform such as GEE, can offer a scalable and efficient framework for long-term urban monitoring. This is particularly impactful in contexts like Ravenna, where updated, high-resolution cartographic resources are scarce. In such data-limited scenarios, the ability to derive accurate land cover classifications using freely available satellite data, coupled with in-platform machine learning tools, represents a cost-effective and operationally viable solution for urban and environmental planners.

The analysis of spatial patterns derived from RF classifications revealed clear urban development trends. The UD indicator showed an increase from 4.49 % in 2000 to 5.73 % in 2024, highlighting a moderate but significant intensification of urban land consumption at the municipal scale. Compared to broader regional trends [22]-[23], Ravenna exhibits a relatively moderate urban density increase. In fact, Ravenna's UD levels in 2024 (5.73 %) remain slightly lower than the average density of approximately 7 % observed across Northern Italy around 2000, suggesting a more contained and structured urban growth. Moreover, per capita urbanisation in Ravenna (approximately 350–400 m² per inhabitant) aligns closely with the regional average of about 360 m² per inhabitant, indicating similar efficiency in land consumption per capita.

The observed growth pattern in Ravenna contrasts sharply with the widespread, dispersed ("sprinkling") pattern identified across the broader Po Valley. Ravenna's urban development has primarily been characterised by planned, consolidated expansion around the historical core and strategic areas such as the port and suburban districts. Despite the presence of fragmented and isolated residential developments, particularly in peripheral zones, the overall pattern suggests relatively controlled growth guided by explicit planning frameworks.

These spatial findings highlight important implications for urban sustainability. The core urban zone's densification through infill supports sustainable land management policies, reduces pressures on surrounding agricultural and natural areas, and helps preserve Ravenna's historical and cultural fabric. However, peripheral expansion still poses challenges related to infrastructure provision, service accessibility, and environmental protection, demanding ongoing monitoring and targeted policy interventions.

One of the key strengths of the proposed methodology is its scalability and transferability. The workflow, developed entirely using open-source tools and the cloud-based GEE platform, is designed for easy replication. This makes it adaptable for application in diverse urban contexts, allowing for comparative studies across regions with varying geographic, socio-economic, and environmental characteristics. Applying this methodology beyond Ravenna could support broader efforts to monitor and quantify urbanisation patterns globally.

While the study successfully demonstrates the applicability of machine learning methods for long-term urban monitoring, several limitations should be acknowledged:

- Spatial resolution constraints: The use of Landsat imagery (30 m resolution) may not capture fine-scale transformations, such as small residential clusters or

narrow transport corridors. For more granular monitoring, higher-resolution datasets, such as Sentinel-2 (10 m) or commercial platforms, should be considered.

- Spectral confusion in complex classes: Despite RF's overall strong performance, some misclassifications occurred between bareland, agriculture, and grass/shrubland. These issues stem from overlapping spectral signatures and highlight the need for more advanced classification techniques in mixed-use zones.
- Algorithmic limitations: Both RF and SVM, while effective, have inherent constraints in handling complex, hierarchical, or contextual features in urban settings. Future work could explore deep learning approaches, such as Convolutional Neural Networks (CNNs), which are better equipped to model non-linear, high-dimensional relationships and may yield improved classification accuracy in spectrally complex environments.

In summary, the integration of GeoAI tools with cloud computing environments provides a robust, flexible, and reproducible framework for measuring and monitoring urban land cover dynamics. The outcomes of this study offer practical insights for urban planning and contribute to the methodological advancement of remote sensing-based urban analytics.

5. CONCLUSIONS

This study presented a GeoAI-based methodology for the measurement and monitoring of urban fabric transformations in the city of Ravenna over a 24-year period (2000–2024). By integrating multispectral satellite imagery, advanced machine learning algorithms, and cloud-based processing on the GEE platform, the proposed approach enhances the geomatics toolkit for LULC monitoring, offering an open-source, replicable approach for territorial analysis and planning.

The comparative evaluation of classification performance, based on F1-score and overall accuracy, confirmed that the RF algorithm consistently outperformed the SVM model across all LULC classes and both reference years. In 2024, RF achieved an overall accuracy of 86 % and high per-class F1-scores, particularly for the built-up, water, and tree cover classes. Notably, McNemar's test confirmed that these differences were statistically significant, reinforcing RF's reliability for operational urban monitoring. The RF classifier also showed superior performance in classifying spectrally complex land cover types, such as bareland and grassland/shrubland, demonstrating its robustness in heterogeneous urban and peri-urban environments.

This methodology enabled the accurate mapping and quantification of spatial changes in key LULC categories, offering measurable indicators of urban growth, land abandonment, and environmental transformation. Its outputs provide robust, reproducible data products that can inform evidence-based planning and support the sustainable management of urban expansion.

Beyond its classification performance, the workflow's scalability and transferability represent key strengths. Developed entirely within an open-source, cloud-based framework, it can be adapted and replicated across diverse geographic, socio-economic, and environmental contexts.

In conclusion, the integration of machine learning, satellite observation, and geospatial analysis within a GeoAI framework offers a powerful toolset for measuring and monitoring urban transformations. By delivering accurate, spatially explicit, and statistically validated data, this approach supports more informed decision-making, encourages sustainable development, and equips urban planners and policymakers to anticipate and respond to evolving territorial challenges.

REFERENCES

[1] V. Chaturvedi, W. T. de Vries, Machine learning algorithms for urban land use planning: A review, Urban Science 5 (2021) 3, 68. DOI: 10.3390/urbansci5030068

[2] M. Samardžić-Petrović, M. Kovačević, B. Bajat, S. Dragićević, Machine learning techniques for modelling short term land-use change, ISPRS International Journal of Geo-Information 6 (2017) 12, 387. DOI: 10.3390/ijgi6120387

[3] M. Francini, C. Salvo, A. Vitale, Combining deep learning and multi-source GIS methods to analyze urban and greening changes, Sensors 23 (2023) 8, 3805. DOI: 10.3390/s23083805

[4] J. Wang, M. Bretz, M. A. A. Dewan, M. A. Delavar, Machine learning in modelling land-use and land cover-change (LULCC): Current status, challenges, and prospects, Science of The Total Environment 822 (2022), 153559. DOI: 10.1016/j.scitotenv.2022.153559

[5] C. Salvo, A. Vitale, Spatiotemporal dynamics of urban growth and greening goals towards sustainable development, in: International Conference on Innovation in Urban and Regional Planning, Springer Nature Switzerland, Cham, 2024, pp. 183–195. DOI: 10.1007/978-3-031-54096-7_17

[6] A. Vitale, C. Salvo, F. Lamonaca, A novel geospatial methodology for measuring and mapping spatiotemporal built-up dynamics based on Google Earth Engine and unsupervised K-means clustering of multispectral satellite imagery, IEEE Int. Workshop on Metrology for Living Environment (MetroLivEnv), Chania, Greece, 12-14 June 2024, pp. 57–62. DOI: 10.1109/metrolivenv60384.2024.10615674

[7] R. Song, Y. Feng, C. Xing, Z. Mu, X. Wang, Hyperspectral image change detection based on active convolutional neural network and spatial-spectral affinity graph learning, Applied Soft Computing 125 (2022), 109130. DOI: 10.1016/j.asoc.2022.109130

[8] A. Velastegui-Montoya, N. Montalván-Burbano, P. Carrión-Mero, H. Rivera-Torres, L. Sadeck, M. Adami, Google Earth Engine: A global analysis and future trends, Remote Sensing 15 (2023) 14, 3675. DOI: 10.3390/rs15143675

[9] Y. Benhammou, D. Alcaraz-Segura, E. Guirado, R. Khaldi, B. Achchab, F. Herrera, S. Tabik, Sentinel2GlobalLULC: A Sentinel-2 RGB image tile dataset for global land use/cover mapping with deep learning, Scientific Data 9 (2022) 1, 681. DOI: 10.1038/s41597-022-01775-8

[10] A. Vitale, C. Salvo, Monitoring and forecasting land cover dynamics using remote sensing and geospatial technology, Italian Conf. on Geomatics and Geospatial Technologies, Springer Nature Switzerland, Cham, 2024, pp. 126–140. DOI: 10.1007/978-3-031-59925-5_10

[11] L. R. Mansaray, F. Wang, J. Huang, L. Yang, A. S. Kanu, Accuracies of support vector machine and random forest in rice mapping with Sentinel-1A, Landsat-8, and Sentinel-2A datasets, Geocarto International 35 (2020) 10, pp. 1088–1108. DOI: 10.1080/10106049.2019.1568586

[12] K. N. Loukika, V. R. Keesara, V. Sridhar, Analysis of land use and land cover using machine learning algorithms on Google Earth Engine for Munneru River Basin, India, Sustainability 13 (2021) 24, 13758. DOI: 10.3390/su132413758

[13] Z. Zafar, M. Zubair, Y. Zha, S. Fahd, A. A. Nadeem, Performance assessment of machine learning algorithms for mapping of land use/land cover using remote sensing data, The Egyptian Journal of Remote Sensing and Space Sciences 27 (2024) 2, pp. 216–226.
DOI: 10.1016/j.ejrs.2024.03.003

[14] M. Weiss, D. Jacob, R. Duveiller, Remote sensing for agricultural applications: A meta-review, Remote Sens. Environ. 236 (2020), 111402.
DOI: 10.1016/j.rse.2019.111402

[15] M. Belgiu, L. Dragu, Random forest in remote sensing: A review of applications and future directions, ISPRS Journal of Photogrammetry and Remote Sensing 114 (2016), pp. 24–31.
DOI: 10.1016/j.isprsjprs.2016.01.011

[16] J. Inglada, A. Vincent, M. Arias, B. Tardy, D. Morin, I. Rodes, Operational high-resolution land cover map production at the country scale using satellite image time series, Remote Sensing 9 (2017), 95.
DOI: 10.3390/rs9010095

[17] M. S. Khan, S. Ullah, L. Chen, Comparison on land-use/land-cover indices in explaining land surface temperature variations in the city of Beijing, China, Land 10 (2021) 10, 1018.
DOI: 10.3390/land10101018

[18] S. Basheer, X. Wang, A. A. Farooque, R. A. Nawaz, K. Liu, T. Adekanmbi, S. Liu, Comparison of land use land cover classifiers using different satellite imagery and machine learning techniques, Remote Sensing 14 (2022) 19, 4978.
DOI: 10.3390/rs14194978

[19] D. Krivoguz, S. G. Chernyi, E. Zinchenko, A. Silkin, A. Zinchenko, Using Landsat-5 for accurate historical LULC classification: A comparison of machine learning models, Data 8 (2023) 9, 138.
DOI: 10.3390/data8090138

[20] S. Puttinaovarat, K. Khaimook, P. Horkaew, Land use and land cover classification from satellite images based on ensemble machine learning and crowdsourcing data verification, International Journal of Cartography (2023), pp. 1–21.
DOI: 10.1080/23729333.2023.2166252

[21] C. Lin, N. D. Doyog, Challenges of retrieving LULC information in rural-forest mosaic landscapes using random forest technique, Forests 14 (2023) 4.
DOI: 10.3390/f14040816

[22] B. Romano, F. Zullo, L. Fiorini, A. Marucci, S. Ciabò, Land transformation of Italy due to half a century of urbanization, Land Use Policy, 67 (2017), pp. 387–400.
DOI: 10.1016/j.landusepol.2017.06.006

[23] B. Romano, F. Zullo, L. Fiorini, S. Ciabò, A. Marucci, Sprinkling: An approach to describe urbanization dynamics in Italy, Sustainability, 9 (2017), 97.
DOI: 10.3390/su9010097